HHS Public Access

Author manuscript

Methods Mol Biol. Author manuscript; available in PMC 2023 January 01.

Published in final edited form as:

Methods Mol Biol. 2022 ; 2419: 645–658. doi:10.1007/978-1-0716-1924-7_40.

Intravital microscopy in atherosclerosis research

Georg Wissmeyer[1], **Mohamad B. Kassab**[1], **Yoichiro Kawamura**[1], **Aaron D. Aguirre**[2], **Farouc A. Jaffer**[1,2,*]

[1]Cardiovascular Research Center, Division of Cardiology, Massachusetts General Hospital, Harvard Medical School, Boston, Massachusetts, USA

[2]Wellman Center for Photomedicine, Harvard Medical School and Massachusetts General Hospital, Boston, MA

Abstract

Atherosclerosis is a lipid-driven inflammatory disorder that narrows the arterial lumen and can induce life-threatening complications from coronary artery disease, cerebrovascular disease and peripheral artery disease. On a mechanistic level, the development of novel cellular-resolution intravital microscopy imaging approaches has recently enabled *in vivo* studies of underlying biological processes governing disease onset and progress. In particular multi-photon microscopy has emerged as a promising intravital imaging tool utilizing two-photon-excited fluorescence and second-harmonic generation that provides sub-cellular resolution and increased imaging depths beyond confocal and epifluorescence microscopy. In this chapter, we describe the state-of-the-art multi-photon microscopy applied to the study of murine atherosclerosis.

Keywords

Atherosclerosis; inflammation; intravital imaging; intravital microscopy; molecular imaging; multi-photon microscopy; gated microscopy

1. Introduction

Atherosclerosis is a chronic inflammatory disease underlying coronary artery disease (CAD) and myocardial infarction, sudden cardiac death, ischemic stroke and peripheral artery disease, and is the leading cause of disability and death worldwide. At present, assessment of pathobiological mechanisms driving atherosclerosis mainly relies on classical histopathology and *ex vivo* studies. However, the pathogenesis of atherosclerosis involves *in vivo* dynamic events driven by cells and molecules that occur over timeframes faster than overall disease progression. Intravital imaging technologies such as multi-photon microscopy (MPM) allow to study disease onset and progression *in vivo* and in real-time, and can therefore help to better understand the underlying biomolecular processes. For example, one of the key goals in atherosclerosis research is to better understand the role of

[*]**ADDRESS FOR CORRESPONDENCE** Farouc Jaffer (fjaffer@mgh.harvard.edu), Address: Massachusetts General Hospital, Cardiovascular Research Center, Simches Research Building, Room 3206, Boston, Massachusetts 02114, Tel (617) 724-9353, Fax (617) 812-7486.

trafficking and resident leukocyte classes in atheroma progression and myocardial infarction healing [1, 2]. In this chapter, we detail the ability to perform *in vivo* MPM in larger arterial vascular disease in murine subjects.

Intravital molecular microscopy (IVM) technologies based on fluorescence contrast are a key pillar of modern biological research, and cellular and sub-cellular resolution approaches such as confocal microscopy (CFM), have enabled the molecular assessment of atherosclerosis in mice *in vivo* [3-5]. Advances in laser technology have led to the development of MPM, where longer excitation wavelengths allow for increased imaging depths of up to 300 μm, compared to around 80 μm in conventional CFM. Moreover, the physical principles of MPM minimize photo-bleaching and out-of-focus absorption, thus vastly decreasing photodamage to the biological specimen [6, 7]. Sophisticated MPM systems allow for simultaneous multi-channel multi-modality image acquisition (e.g. via two-photon-excited fluorescence (2PEF)) of various fluorescent dyes/proteins and of non-linear optical microscopy techniques (i.e. second-harmonic generation (SHG) and third-harmonic generation (THG)) [8]. These capabilities are particularly attractive for comprehensive imaging of associated biomolecular processes in atherosclerosis, where cell types of interest may be individually labelled and imaged via dedicated channels acquired separately from channels dedicated to imaging surrounding tissue substructure such as collagen via SHG and THG contrast [9]. With asset costs and complexity of MPM systems steadily decreasing, multi-modal IVM is set to become accessible to a fast-growing biological research-community and will lead to a significant improvement to the study of atherosclerosis.

A commonly used animal model for atherosclerosis research is the Apolipoprotein E knockout ($ApoE^{-/-}$) mouse in combination with a Western-type diet (high fat and cholesterol content). As of today, no mouse model to date can fully recapitulate every pathophysiological aspect of human atherosclerosis. However, a variety of transgenic mouse models have been established in the past decades allowing for example to investigate lipid metabolism in early phase atherosclerosis or to study plaque vulnerability in an advanced atherosclerosis [10, 11]. However in common mouse models, atherosclerotic plaques develop in vessels such as the brachiocephalic or carotid arteries [12] that are not suitable for conventional intravital microscopy, either because of the need for highly invasive surgery and/or due to artifacts induced by cardiac and respiratory motion. This is of particular relevance for MPM, where both in-plane and through-plane motion can affect image quality [13-15]. In the case of the carotid artery, mechanical stabilization of the artery relative to the microscopy setup (e.g. via spatially fixated coverslips) allows for real-time IVM microscopy. However, any kind of mechanical- or pressure-based fixation may alter native physiology (e.g. by altering flow and leukocyte recruitment) and may therefore not be physiologically relevant. A promising approach for motion-compensated IVM leverages gating technologies (i.e. via cardio-respiratory synchronization with the IVM image acquisition) [16]. However, gated imaging requires sophisticated hardware and software, and off-the-shelf IVM systems for gated acquisition are not commercially available yet.

In this chapter, we detail a method for performing intravital MPM on a large-caliber vascular disease model that reflects the current possibilities of IVM microscopy. The

described method is fully transferable to gated MPM of murine carotid atherosclerosis but is introduced based on established protocols and commercially available hardware, utilizing a thrombosis model, to demonstrate leukocyte trafficking, as relevant to atherosclerosis pathobiology [17].

2. Materials

The selection of microscope settings (i.e. excitation wavelengths and emission filters) as well as the selection of endogenous and/or exogenous fluorescence labels/agents depends on the specific molecular and/or cellular target(s) to be investigated in the study (*see* Note 1). Exogenous fluorophore solutions should be prepared right before procedure and remain protected from light.

2.1. Multi-Photon Microscope

1. Sophisticated multi-photon microscopy (MPM) suites for high-speed 2D and 3D multi-modal image acquisition are provided by multiple manufacturers with similar specifications and one commercially available MPM system is the FVMPE-RS (Olympus, Japan). The microscope employs two tunable broad bandwidth lasers for excitation wavelengths ranging from 680 nm to 1300 nm and a set of four corresponding photo multiplier tubes (PMTs) for simultaneous 4-channel imaging. A broad excitation bandwidth and respective optical dichroic/filter system allows for SHG and THG as well as for simultaneous imaging of dye- and protein-based fluorophores (*see* Note 2).
2. Scanning is performed with a set of galvanometer and resonant scanning mirrors in combination with a piezo-driven z-stage for the objective.
3. A water immersion objective dedicated for multiphoton excitation such as the XLPLN25XWMP2 (Olympus, Japan) is applied with a magnification of 25x, a working distance of 2 mm and a numerical aperture (NA) of 1.05 (*see* Note 3).
4. The MPM may only be equipped with a bright-field eyepiece for sample alignment. However, a digital camera for acquiring bright-field microscopy images, particularly for serial studies, is useful.
5. 3D adjustment of the specimen (i.e. the mouse model) can be performed with XYZ stages implemented into the microscope and/or with a set of additionally mounted stages (*see* Note 4).
6. Sophisticated analysis of 2D images and 3D image stacks can be performed with ImageJ image processing software (v. 1.53f, freeware, NIH https://imagej.nih.gov/ij/download.html) (*see* Note 5).

2.2. Exogeneous Fluorophores

1. Dilution of imaging agnts: Depending on manufacturer specifications, phosphate buffered saline (1x PBS) or 0.9% (normal) saline solutions are used.

2. Blood microcirculation and negative cell contrast: Fluorescein isothiocyanate (FITC)-dextran (MW 2,000,000). Excitation/Emission 490/520 nm. Solution prepared at a dosage of 25-50 mg/kg.

3. Leukocyte and platelet labeling [18]: Rhodamine 6G. Excitation/Emission 528/552 nm. Solution prepared at a dosage of 2.5 mg/kg.

4. More specific and comprehensive cell labeling can be achieved with genetically-encoded fluorescent tags (e.g. green fluorescence protein (GFP)) or antibody-based labeling, including for neutrophils (e.g. a phycoerythrin-conjugated antibody to Ly6G, clone 1A8) and for cell nuclei (e.g. 4′,6-diamidino-2-phenylindol).

2.3. Murine model

1. Mouse model: In our experiment C57BL/6J male mice, aged between 13-17 weeks were used. However, any mouse type (C57BL/6J, ApoE−/−, LDLr−/−, etc.) could be employed.

2. Surgical setup: Standard rodent animal surgical equipment for vascular dissection; nylon suture for ligation (7-0, 0.5 metric, black monofilament); stereomicroscope.

3. Inhalational anesthesia: 1% to 2% isoflurane. When the MPM does not allow incorporation of an inhalational anesthesia setup, use intraperitoneal Ketamine/xylazine injection at a dosage of 80/12 mg/kg.

4. Homeothermic monitoring system: Closed loop body temperature control system for mouse model with heating pad sized according to the microscopy setup.

5. Intraorbital Injection: A 27-gauge needle with a 1 ml syringe attached.

2.4. Epifluorescence microscope

1. A commercially available epifluorescence microscope (EFM) is the Nikon Eclipse 90i (Nikon Imaging, Japan). It allows for real-time microscopy (image and video acquisition) in samples ranging from thin tissue to small animals. Illumination wavelengths are selected via a range of filter sets (e.g. allowing for excitation in the FITC channel at 475/35 nm).

2. The selected lower-magnification EFM allows for fluorescence and bright-field imaging to provide a rapid roadmap for fluorescence signals, which is particularly useful for facilitating MPM studies, as it provides a “big picture” view of labelled vascular pathology, and allows one to focus on specific regions for high-resolution high-magnification MPM studies.

3. Software for image acquisition and analysis is provided by the manufacturer (Nikon, i-Series control software) (*see* Note 5).

3. Methods

As a prelude to murine atherosclerosis studies employing anticipated commercially available gating software in the future, a murine deep venous thrombosis (DVT) model is established in the femoral/saphenous vein and induced by combined ligation (flow restriction) and light irradiation [19]. This model generates rapid platelet and leukocyte trafficking in a model relevant to human stasis DVT, as well as atherothrombosis. Intravital MPM is then performed with two-photon excitation fluorescence (2PEF) in the selected channels for functional imaging as well as in the SHG channel for monitoring vessel morphology via collagen. Labeled platelets and leukocytes accumulate at the freshly induced thrombus which is observable (e.g. as negative contrast following FITC dextran injection). In contrast to CFM, MPM offers prolonged imaging without photobleaching at greater imaging depths while providing 2D and 3D image acquisition at high frame rates. The step-by-step methods are explained in the following sections

3.1. Mouse preparation

1. Obtain institutional animal committee approval for planned experiments and follow animal handling protocols that apply at your laboratory.
2. Induce inhalational anesthesia (1% to 2% isoflurane) if applicable or induce anesthesia with Ketamine/xylazine injection (IP, 80/12 mg/kg). Inject maintenance doses when necessary and in conjunction with laboratory protocol (e.g. every 30-45 minutes; *see* Note 6).
3. Immobilize and fixate mouse in dorsal position on a mobile platform (*see* Note 4). Supply external heating to 37°C as necessary.
4. Applying the surgical setup, make a surgical incision longitudinally from the mid-inguinal ligament to the knee. Excise the exposed body of adipose tissue and connective tissue to permit vessel exposure of femoral/saphenous vein and artery.
5. Separate the femoral vein carefully from the concomitant femoral artery and nerve proximal of the venous bifurcation, and ligate with a nylon suture to induce complete vessel occlusion, resulting in marked decrease in blood flow at the saphenous vein [19] (*see* Note 7).
6. Intraorbital injection is employed by gently applying pressure onto the left peri-orbital area and exposing the left eye. A 27-gauge needle with a 1 ml syringe which was attached into the orbital venous sinus with the needle facing forward at a 45° angle. Inject desired molecular, cellular and angiographic imaging agents as detailed next and permit circulation for 10 minutes prior to imaging.
7. To visualize the blood lumen of target arteries and veins, inject the exogenous fluorophore FITC-dextran via intravenous or retro-orbital injection, and permit circulation for 10 minutes prior to imaging.
8. To visualize circulating and trafficking leukocytes and platelets, co-inject the exogenous fluorophore Rhodamine 6G in the same manner as FITC-dextran.

9. Transfer mouse to the MPM suite while keeping the femoral artery surgically exposed but moist and light-protected.

3.2. Thrombus model

1. On the EFM microscope, choose a relatively high NA objective lens with increased irradiance for thrombus formation (e.g. Nikon Plan Fluor, 10x, NA 0.3). Choose objective lens for larger region-of-interest (ROI) when (bright-light) imaging (Nikon Plan Fluor, 4x, NA 0.13).
2. Localize and determine a suitable region of interest (ROI) of the saphenous vein (area with minimal branching) using bright-light microscopy at the lowest reasonable intensity setting to avoid photobleaching. Centralize the field of view (FOV) in the ROI and match the axial position of the focal plane around 100 μm below the vessel dome along the Z axis. Record this FOV position in advance for MPM imaging.
3. Apply fluorescence imaging in the FITC-channel (Excitation 475/35 nm) over the ROI as long as necessary to induce thrombus formation via light irradiation. Adjust light intensity directly or by ND filter settings to around 2.5 mW (*see* Note 8).
4. Observe thrombus induction and formation in the EFM image feed and halt irradiation once thrombus reaches desired extent and/or volume (Figure 1) [20].
5. Transfer mouse to the MPM suite and keep the vein surgically exposed as well as moist and light-protected.

3.3. Multiphoton Microscopy

1. Place the surgically-exposed animal into the MPM setup and situate the equipment for fixation, body heating and anesthesia. Position and orient the animal to match the capabilities of the MPM system (*see* Note 9). Apply optical matching medium onto the ROI and couple the water immersion objective (*see* Note 10).
2. Localize the ROI determined on the EFM with bright-light microscopy or by direct observation via the eyepieces. Conduct a first 2PEF scan in the FITC channel to match the FOV with the desired ROI (i.e. the proximal edge of thrombus formation). Adjust the focal plane axially (i.e. to 100 μm below the vessel dome; anterior topmost surface).
3. Select target fluorescence channels by adjusting the wavelength(s) of the excitation laser(s) and the respective PMT channel. Select filters or filter sets according to the targeted fluorescence and SHG/THG channels (*see* Note 11). Utilizing live image read-out, fine-tune acquisition settings for each channel (i.e. laser intensity, sensitivity, gain and offset) (*see* Note 12).
4. Adjust the scan size of the ROI and the scan speed for image acquisition. Slower scan speeds usually increase SNR while minimized scan areas and fast scan speeds are favorable for live imaging of leukocyte dynamics.

5. Acquire 2D data (i.e. images of stacks with multiple channels simultaneously, in single shot or continuous mode) (Figure 2). Fine-tune image settings as needed to compensate for varying contrast inherent to the sample or caused by photobleaching.

6. For 3D image acquisition, use 2D scans to find the upper and lower boundaries of the focal planes accessible. Adjust the focal plane axially to match the vessel dome to determine the upper boundary as primary reference point. Determine the lower boundary as the axial plane where signal strength and resolution are yet undistorted. Set boundaries for scanning Z series accordingly and choose step size depending on whether high acquisition speed or high definition data is desired.

7. Acquire 3D data by performing a Z series scan. Adjust spatial scan dimensions to improve acquisition performance and record relevant 3D data [21] (Figure 3).

8. The study of atherosclerosis or thrombosis induced in larger arteries (e.g. in the carotid artery) for 2D and 3D image acquisition may be impeded by tissue movement (i.e. by cardiac and respiratory movement). If available, apply cardio-respiratory synchronization with prospective gating to overcome this limitation [16] (*see* Note 13).

3.4. MPM Image Analysis

1. The Olympus MPM software comes with potent tools for image analysis and data management. For image analysis independent of the MPM platform, ImageJ has been established as freely accessible standard software.

2. Export or transfer data to a format accessible by ImageJ or use a Plugin provided by the manufacturer to convert the format (*see* Note 5). Similar to TIFF images, the Olympus OIR image format stores data as hyperstack. Sort the data depending on the study at hand (e.g. by rearranging images acquired in a specific channel or by excluding another channel from the data set).

3. Use ImageJ functionality (z-Project) or plugins (3D Viewer, Volume Viewer) to create 3D visualizations of the loaded stack.

4. Use ImageJ ROI tool to measure the signal intensity at a specific point or the average signal intensity in a specific area as well as in a region without or with little apparent signal (background). Use this data to determine the respective SNR in each channel or the overall SNR for a given Z stack.

3.5. Correlative fluorescence microscopy

1. Perform correlative fluorescence microscopy of fresh-frozen cryocut sections (*see* Note 14) of the thrombus model to corroborate MPM data (e.g. the localization of fluorophores to specific cells and regions) as this step is critical for result interpretation. Moreover, it allows deeper assessment of areas below the depth-sensing capability of MPM (i.e. depths >80-100 μm).

2. Perfuse the femoral/saphenous vein after sacrifice by gently injecting 20 mL of cold PBS from the left ventricle. Then excise the femoral/saphenous vessels with their surrounding tissue and directly embed as fresh-frozen tissue into optimal cutting temperature compound and suspend to −80°C.

3. Cryocut serial 5-10 μm sections of fresh-frozen excised sample and transfer to a dedicated confocal fluorescence microscope or EFM (*see* Note 14).

4. Acquire fluorescence images in the respective channels used during MPM and/or in endogenous and exogenous channels of histology labels (*see* Note 15).

5. Correlate histopathology to confirm specificity of functional and morphological data obtained by MPM.

4 Notes

1. Prior to planning the studies, it is important to observe that the selection of fluorophores for 2PEF matches the laser excitation in MPM/2PEF. The upper wavelength cut-off of around 1300 nm (depending on the system and/or manufacturer) commonly comes hand-in-hand with decreasing laser power at higher wavelengths. While theoretically enabling the use of fluorophores with excitation wavelengths of up to 650 nm, the utilization of fluorophores for 2PEF above around 600 nm should be carefully matched to the spectral distribution of laser power at hand. Alternatively, excitation wavelengths in the high visible range and the NIR may be utilized for single photon absorption fluorescence for such fluorophores if the MPM/ the optical system layout allows for it.

2. In contrast to CFM and epifluorescence microscopes, commercial MPM setups may require guidance/service through the manufacturer when refitting respective dichroic/filter elements/sets to avoid damage (e.g. to the PMTs).

3. A lower magnification objective (e.g. 10x) may be applied to achieve longer working distances, albeit at lower photon collection rate and reduced SNR. Objectives with longer working distances may be selected to help acquire images in a given ROI of a specimen that would otherwise be spatially inaccessible (e.g. when laterally masked by the abdomen in a mouse model). For imaging thin specimen prepared with cover glass as well as deep tissue ROIs in intravital studies on the same setup, an objective with correction ring should be selected (e.g. for correcting 0 – 0.23 mm of cover glass).

4. The MPM system might not come equipped with an XYZ stage suitable for intravital imaging (e.g. in terms of axis movement). Here, a set of (additional) manual XY(Z) stages fixated atop the XYZ platform inherent to the MPM system may allow for reproducible sample orientation, serial studies and movement between spatially separated ROIs. Such a removable platform may also be used for the permanent installation of equipment necessary for animal handling (i.e. mouse fixation), animal heater system and tubing for isoflurane anesthesia.

5. Most manufacturers provide software for the conversion of image file types. Olympus provides a plugin for ImageJ to load vsi/oir/omp2info file formats accessible e.g. at https://imagej.net/OlympusImageJPlugin). Nikon provides a plugin for ImageJ to load nk2 file formats accessible e.g. at https://imagej.nih.gov/ij/plugins/nd2-reader.html.

6. In case isoflurane gas anesthesia is utilized, be aware of increased image artifacts caused by arterial pulsation due to the vasodilatory actions of isoflurane.

7. For survival studies and to keep the target thrombus or atheroma physiologically preserved, minimal amounts of PBS or deionized (DI) water need to be applied to the tissues throughout the procedure to keep moist.

8. Depending on the mouse model, the EFM light source, the duration of EFM illumination and other variables and the duration for thrombus induction will vary and can take up to several minutes. For example, an irradiation of 6 mW/mm^2 will cause thrombus induction at around 3-4 minutes. Record irradiation duration and power to find the optimal ratio between illumination power setting and irradiation duration in an iterative process and adjust settings according to your system parameters.

9. MPM systems commonly exhibit “slow” and “fast” axis modes, giving the possibility to select between high definition (galvo) and high speed (resonant) scanning, respectively. This may affect acquisition speed of individual ROIs and it is important to orientate the animal accordingly prior to imaging and to, for example, match the “fast” axis with the lateral orientation of the target vessel.

10. Deionized (DI) water tends to evaporate quickly and needs to be reapplied periodically for prolonged imaging. An alternative optical matching medium to DI water is lubricant eye gel (GenTeal, Alcon, Switzerland). Another alternative to DI water is isotonic saline solution or PBS, as water can cause tissue swelling due to osmotic shifts.

11. Depending on how sophisticated the applied MPM is, wavelength and filter selection can be performed indirectly by a dye selector embedded in the control software.

12. Unnecessary photo-bleaching can be avoided by fine-tuning channel parameters in a region adjacent to the ROI (i.e. at the distal end of the thrombus). When fine-tuning, avoid sensor-saturation and adjust laser and PMT settings to maximize dynamic range. Save acquisition settings for subsequent imaging of similar models.

13. Minor vessel motions may be minimized by using a mechanical stabilizer, such as a fixated cover glass. For imaging major arteries or when imaging at ROIs inflicted by respiratory movement, gating triggered by mechanical ventilation and cardiac pacing can be considered. Note that non-surgical models of atherosclerotic plaques visualizing the behvaior of leukocytes in atherosclerotic branches in murine carotid artery have been reported. Here, the intravital

microscope combined cardiac triggering and image postprocessing to correct for motion artifacts [22, 23].

14. Fresh-frozen cryocut sectioning: After sacrifice, DVT and control sections of the vessels are harvested, thoroughly washed in PBS, and frozen in an optimal cutting temperature compound on dry ice. The frozen tissue is then cut into 5-10 μm thick sections using an embedded cryocutting microscopy system. Sections are placed on microscopy slides on assessed by fluorescence microscopy, or air-dried and processed for histological and immunohistochemistry staining.

15. Histology labels are, for example, hematoxylin and eosin (H&E stain) for general morphology and the Carstair's method for staining collagen as well as visualizing vessel wall morphology.

Acknowledgments:

The authors are grateful to Emily Cronin-Furman, Ph.D., for helpful discussions on multiphoton microscopy.

Funding:

The work presented in this chapter was funded in part by grants NIH R01 HL150538 and R01 HL137913 to F.A.J..

References:

1. Mulder WJM, Jaffer FA, Fayad ZA, Nahrendorf M (2014) Imaging and nanomedicine in inflammatory atherosclerosis. Sci Transl Med 6:1–12. 10.1126/scitranslmed.3005101
2. Badimon L, Vilahur G (2014) Thrombosis formation on atherosclerotic lesions and plaque rupture. J Intern Med 276:618–632. 10.1111/joim.12296 [PubMed: 25156650]
3. Brown EB, Campbell RB, Tsuzuki Y, Xu L, Carmeliet P, Fukumura D, Jain RK (2001) *In vivo* measurement of gene expression, angiogenesis and physiological function in tumors using multiphoton laser scanning microscopy. Nat Med 7:864–868 [PubMed: 11433354]
4. Jaffer FA (2011) Intravital fluorescence microscopic molecular imaging of atherosclerosis. Methods Mol Biol 680:131–140. 10.1007/978-1-60761-901-7_9 [PubMed: 21153378]
5. Choi M, Kwok SJJ, Yun SH (2015) *In vivo* fluorescence microscopy: Lessons from observing cell behavior in their native environment. Physiology 30:40–49. 10.1152/physiol.00019.2014 [PubMed: 25559154]
6. Taqueti VR, Jaffer FA (2013) High-resolution molecular imaging via intravital microscopy: Illuminating vascular biology *in vivo*. Integr Biol (United Kingdom) 5:278–290. 10.1039/c2ib20194a
7. Ntziachristos V (2010) Going deeper than microscopy: the optical imaging frontier in biology. Nat Methods 7:603–614. 10.1038/nmeth.1483 [PubMed: 20676081]
8. Zipfel WR, Williams RM, Webb WW (2003) Nonlinear magic: multiphoton microscopy in the biosciences. Nat Biotechnol 21:1369–1377. 10.1038/nbt899 [PubMed: 14595365]
9. Megens RTA, Reitsma S, Schiffers PHM, Hilgers RHP, De Mey JGR, Slaaf DW, oude Egbrink MGA, van Zandvoort MAMJ (2007) Two-photon microscopy of vital murine elastic and muscular arteries: Combined structural and functional imaging with subcellular resolution. J Vasc Res 44:87–98. 10.1159/000098259 [PubMed: 17192719]
10. Oppi S, Lüscher TF, Stein S (2019) Mouse models for atherosclerosis research—Which is my line? Front Cardiovasc Med 6:1–8. 10.3389/fcvm.2019.00046 [PubMed: 30740396]
11. Breslow JL (1996) Mouse models of atherosclerosis. Science (80-) 272:685–688. 10.1126/science.272.5262.685

12. Emini Veseli B, Perrotta P, De Meyer GRA, Roth L, Van der Donckt C, Martinet W, De Meyer GRY(2017) Animal models of atherosclerosis. Eur J Pharmacol 816:3–13. 10.1016/j.ejphar.2017.05.010 [PubMed: 28483459]

13. Maresca D, Jansen K, Renaud G, den Dekker W, van Soest G, Li X, Zhou Q, Cannata J, Shung KK, van der Steen AFW (2012) Intravascular ultrasound chirp imaging. Science (80-) 043703:10–13. 10.1063/1.3679375

14. Rademakers T, Douma K, Hackeng TM, Post MJ, Sluimer JC, Daemen MJAP, Biessen EAL, Heeneman S, van Zandvoort MAMJ (2013) Plaque-associated vasa vasorum in aged apolipoprotein E-deficient mice exhibit proatherogenic functional features *in vivo*. Arterioscler Thromb Vasc Biol 33:249–256. 10.1161/ATVBAHA.112.300087 [PubMed: 23241413]

15. Megens RTA, Bianchini M, Schmitt MMN, Weber C (2015) Optical imaging innovations for atherosclerosis research: Multiphoton microscopy and optical nanoscopy. Arterioscler Thromb Vasc Biol 35:1339–1346. 10.1161/ATVBAHA.115.304875 [PubMed: 25908769]

16. Vinegoni C, Aguirre AD, Lee S, Weissleder R (2015) Imaging the beating heart in the mouse using intravital microscopy techniques. Nat Protoc 10:1802–1819. 10.1038/nprot.2015.119 [PubMed: 26492138]

17. Haka AS, Potteaux S, Fraser H, Randolph GJ, Maxfield FR (2012) Quantitative analysis of monocyte subpopulations in murine atherosclerotic plaques by multiphoton microscopy. PLoS One 7:. 10.1371/journal.pone.0044823

18. Herr N, Mauler M, Bode C, Duerschmied D (2015) Intravital microscopy of leukocyte-endothelial and platelet-leukocyte interactions in mesenterial veins in mice. J Vis Exp 2015:1–6. 10.3791/53077

19. Okano M, Hara T, Nishimori M, Irino Y, Satomi-Kobayashi S, Shinohara M, Toh R, Jaffer FA, Ishida T, Hirata K (2020) *In vivo* imaging of venous thrombus and pulmonary embolism using novel murine venous thromboembolism model. JACC Basic to Transl Sci 5:344–356. 10.1016/j.jacbts.2020.01.010

20. Jaffer FA, Kim DE, Quinti L, Tung C-H, Aikawa E, Pande AN, Kohler RH, Shi GP, Libby P, Weissleder R (2007) Optical visualization of cathepsin K activity in atherosclerosis with a novel, protease-activatable fluorescence sensor. Circulation 115:2292–2298. 10.1161/CIRCULATIONAHA.106.660340 [PubMed: 17420353]

21. Li W, Luehmann HP, Hsiao H-M, Tanaka S, Higashikubo R, Gauthier JM, Sultan D, Lavine KJ, Brody SL, Gelman AE, Gropler RJ, Liu Y, Kreisel D (2018) Visualization of monocytic cells in regressing atherosclerotic plaques by intravital 2-photon and positron emission tomography–based imaging—Brief Report. Arterioscler Thromb Vasc Biol 38:1030–1036. 10.1161/ATVBAHA.117.310517 [PubMed: 29567678]

22. McArdle S, Chodaczek G, Ray N, Ley K (2015) Intravital live cell triggered imaging system reveals monocyte patrolling and macrophage migration in atherosclerotic arteries. J Biomed Opt 20:1. 10.1117/1.JBO.20.2.026005

23. Chèvre R, González-Granado JM, Megens RTA, Sreeramkumar V, Silvestre-Roig C, Molina-Sanchez P, Weber C, Soehnlein O, Hidalgo A, Andres V (2014) High-resolution imaging of intravascular atherogenic inflammation in live mice. Circ Res 114:770–779. 10.1161/CIRCRESAHA.114.302590 [PubMed: 24366169]

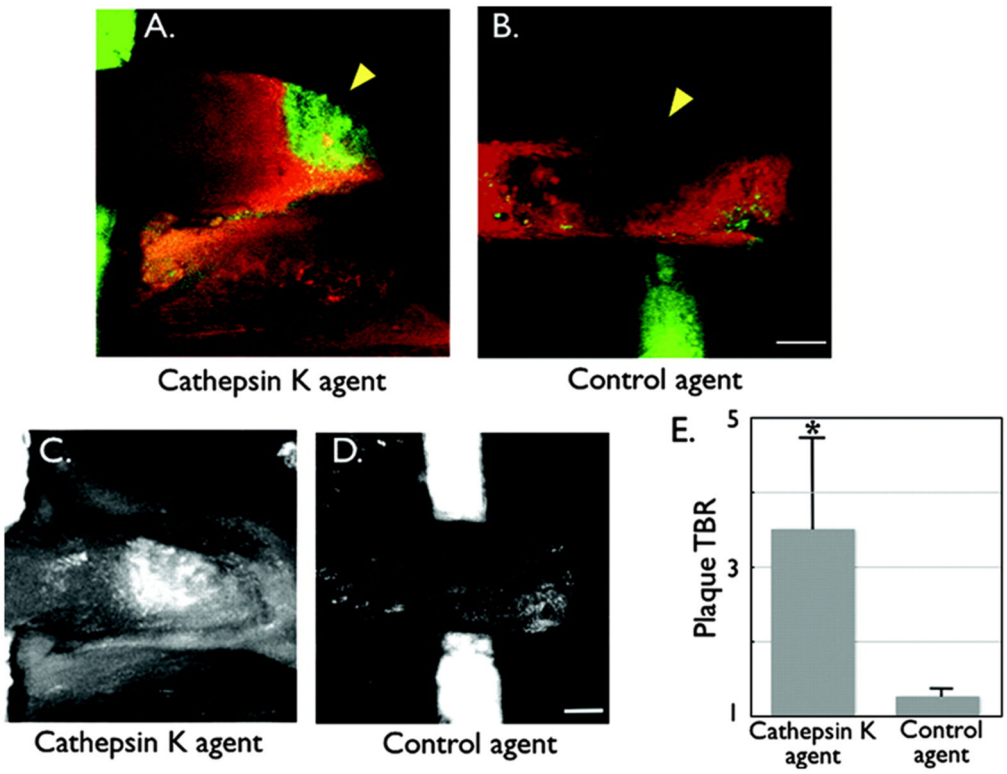

Figure 1: *In vivo* imaging of Cathepsin K (CatK) activity in carotid atherosclerotic plaques of ApoE$^{-/-}$ mice.

Atheroma were surgically exposed and then underwent laser scanning intravital fluorescence microscopy 24 hours after injection of the CatK or control K imaging agent (5 nmol). Multiwavelength imaging allowed detection of the CatK signal and a spectrally resolved intravascular agent injected just before imaging. A cylindrical Cy5.5 dye-filled phantom (green) was placed under the carotid artery to facilitate localization. A) Fusion *in vivo* image of a carotid vessel (×5 magnification; 13×13-μm in-plane resolution; 10-μm slice thickness) demonstrating focal CatK signal (green) in an atherosclerotic lesion (arrowhead). The lesion was confirmed to be within the vascular space as defined by the intravascular agent (red). B) Fusion image of a carotid plaque (arrowhead) in the control group demonstrating minimal NIRF signal in the CatK channel. The plaque appears as a signal void or filling defect within the vascular space. C) and D) Projection images of the carotid plaques after injection of the CatK imaging agent (C) or control agent (D), demonstrating greater plaque TBRs (E) in the CatK vs control group (*P<0.05). Projection images processed and windowed identically. Scale bar, 250 μm.

Reproduced from ref. [20] with permission from Wolters Kluwer Health, Inc.

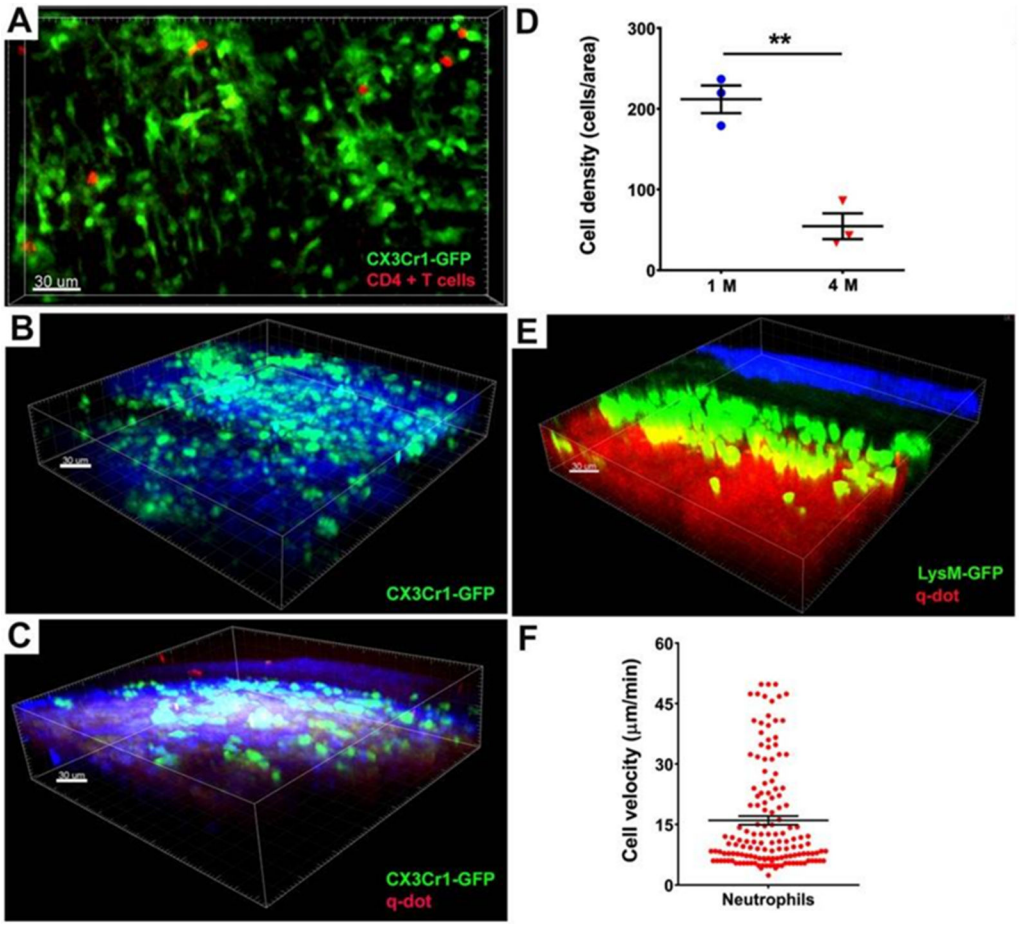

Figure 2: Intravital two-photon imaging and PET-based scanning reveal immune cell behavior in aortic arch grafts.

A) Representative picture showing monocytes/macrophages (green) and CD4+ T cells (red) in CBA aortic arch grafts 1 week after transplantation into B6 CX3CR1 GFP/+ mice (n=3) (GFP, green fluorescent protein). Male → male strain combination is depicted in this figure. Monocytes / macrophages (green) in male B6 ApoE$^{-/-}$ aortic arch grafts (B) 1 month (n=3) and (C) 4 months (n=3) after transplantation into male B6 CX3CR1 GFP/+ mice. D) Reduction of density of CX3CR1 GFP+ cells within regressing plaques (212 ± 17 cells/area (220 x 240 µm2) at 1 month (blue) vs. 54 ± 16 cells/area at 4 months (red), n=3, **p < 0.01). E) Representative image of male B6 ApoE$^{-/-}$ aortic arch grafts transplanted into male B6 LysM-GFP mice 1 day after engraftment (n=3). Collagen appears blue due to second harmonic generation. Blood vessels are labeled red after injection of quantum dots. Scale bars, 30 µm. F) Velocity of LysM-GFP cells in male B6 ApoE$^{-/-}$ aortic arch grafts 24 hours after engraftment (mean velocity is 16.02 µm/min ± 1.08; analyzed cells pooled from 3 independent experiments.

Reproduced from ref. [21] with permission from Wolters Kluwer Health, Inc.

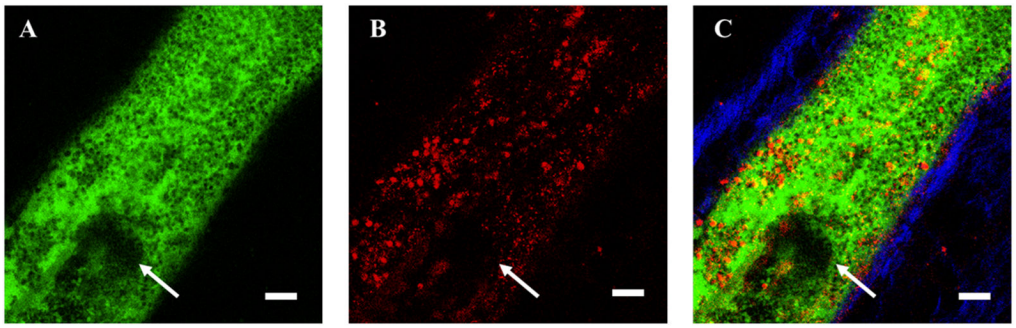

Figure 3: Proximal edge of am acute stasis deep vein thrombosis (DVT) formed in the murine saphenous vein following, fluorescin isothiocyanate (FITC) injection and FITC-based light illumination for 60 seconds.

A) FITC-dextran (green) image of vessel lumen and thrombus (white arrow) and leukocytes appearing as negative-contrast. B) Leukocytes and platelets visualized by Rhodamine 6G (red) injected after FITC-light thrombus induction. C) Merged FITC-dextran, Rhodamine 6G and SHG (blue) signals, with SHG visualizing primarily type I collagen in the vessel wall. Scale bar, 50 μm.